

9-1-2017

## Addressing a Common Misconception: Ammonium Acetate as Neutral pH "Buffer" for Native Electrospray Mass Spectrometry.

Lars Konermann

Follow this and additional works at: <https://ir.lib.uwo.ca/chempub>

 Part of the [Chemistry Commons](#)

---

### Citation of this paper:

Konermann, Lars, "Addressing a Common Misconception: Ammonium Acetate as Neutral pH "Buffer" for Native Electrospray Mass Spectrometry." (2017). *Chemistry Publications*. 261.  
<https://ir.lib.uwo.ca/chempub/261>

Invited “Critical Insights Review”

for *J. Am. Soc. Mass Spectrom.*

**Addressing A Common Misconception: Ammonium Acetate as  
Neutral pH “Buffer” for Native Electrospray Mass Spectrometry**

Lars Konermann\*

*Department of Chemistry, The University of Western Ontario, London, Ontario, N6A 5B7,  
Canada*

**Running Title:** Buffers in Native ESI-MS

\* To whom correspondence should be addressed. Telephone: (519) 661-2111 ext. 86313.

Email: [konerman@uwo.ca](mailto:konerman@uwo.ca)

**Abstract.** Native ESI-MS involves the transfer of intact proteins and biomolecular complexes from solution into the gas phase. One potential pitfall are pH-induced changes experienced by the analyte while it is still surrounded by solvent. Most native ESI-MS studies employ neutral aqueous ammonium acetate solutions. It is a widely perpetuated misconception that ammonium acetate buffers the analyte solution at neutral pH. By definition, a buffer consists of a weak acid and its conjugate weak base. The buffering range covers the weak acid  $pK_a \pm 1$  pH unit.  $NH_4^+$  and  $CH_3-COO^-$  are not a conjugate acid/base pair, which means that they do not constitute a buffer at pH 7. Dissolution of ammonium acetate salt in water results in pH 7, but this pH is highly labile. Ammonium acetate does provide buffering around pH 4.75 (the  $pK_a$  of acetic acid) and around pH 9.25 (the  $pK_a$  of ammonium). This implies that neutral ammonium acetate solutions electrosprayed in positive ion mode will likely undergo acidification down to  $pH 4.75 \pm 1$  in the ESI plume. Ammonium acetate remains a useful additive for native ESI-MS. It is a volatile electrolyte that can mimic the solvation properties experienced by proteins under physiological conditions. Also, a drop from pH 7 to around pH 4.75 is less dramatic than the acidification that would take place in pure water. It is hoped that the habit of referring to pH 7 solutions as ammonium acetate “buffer” will disappear from the literature. Ammonium acetate “solution” should be used instead.

**Keywords:** Henderson-Hasselbalch equation; dissociation equilibrium; acid/base chemistry; droplet evaporation; noncovalent complexes in the gas phase.

## Introduction

Native electrospray ionization (ESI) mass spectrometry (MS) is a versatile tool for probing the structure and composition of proteins, protein-ligand complexes, all the way to MDa biomolecular assemblies [1-9]. This area has experienced significant growth in recent years, fuelled by the development of instruments that are capable of performing both  $m/z$  analyses and ion mobility measurements [10-15]. For native ESI-MS the analytes are dissolved in a non-denaturing solvent, usually aqueous ammonium acetate ( $\text{NH}_4^+ \text{CH}_3\text{-COO}^-$ ) at neutral pH [16]. Regular or nanoESI are used to spray the solution directly into the ion sampling interface. This article takes a critical look at the properties of ammonium acetate in a native ESI-MS context. In particular, we scrutinize the widely repeated claim that ammonium acetate acts as a “buffer” at neutral pH. For putting this issue into context, we will initially discuss aspects related to protein stability in solution and in the gas phase, as well as factors that can induce pH changes during the ESI process.

## Proteins in Aqueous Solution

Proteins have evolved in an aqueous environment. Many of their biological functions involve noncovalent contacts with other proteins, nucleic acids, or membranes. Biomolecular structures and interactions are stabilized by intricate networks of hydrogen bonds, hydrophobic contacts, and electrostatic linkages (salt bridges, charge-dipole interactions, van der Waals forces, etc.) [17]. The aqueous environment is an integral part of this interaction network. Unfavorable contacts between water and nonpolar sites cause proteins to form a hydrophobic core [18,19]. The high dielectric constant of water ( $\kappa_e \approx 80$ ) results in screening effects, such that electrostatic interactions are much weaker than in the vacuum where  $\kappa_e = 1$  [20,21]. This water-mediated screening is further amplified by dissolved electrolytes [22], keeping in mind that physiological ionic strength is around 150 mM [23].

The acid/base milieu is a critical factor for protein stability in solution. Intracellular pH values around 7 are maintained by various buffer systems including  $\text{CO}_2/\text{H}_2\text{CO}_3/\text{HCO}_3^-$ , and by transmembrane ion transporters [24,25]. A stable pH is essential because proteins possess titratable sites that alter their charge depending on pH [26,27]. pH-induced changes of charge patterns can cause deactivation, unfolding, and precipitation [26,27]. Often these effects are related to the release of metal cofactors, triggered by side chain protonation. Histidines are particularly prone to protonation due to their  $\text{pK}_a$  values around 7, but Asp and Glu ( $\text{pK}_a \sim 4$ ) can also be involved [28]. In an effort to mimic the intracellular environment, classical biochemical experiments are generally conducted in neutral aqueous solutions that contain background electrolytes, as well as a buffer system to stabilize pH (e.g., 150 mM NaCl with 25 mM sodium phosphate buffer at pH 7) [27,29].

### **Transferring Native-Like Proteins from Solution into the Gas Phase**

The development of ESI in the late 1980s for the first time allowed the transfer of proteins from solution into the gas phase, making them amenable for analyses by MS as intact  $[\text{M} + z\text{H}]^{z+}$  ions [30]. Soon afterwards it became apparent that even protein-ligand and protein-protein complexes can be studied using this approach [31-33]. The preservation of noncovalent complexes sparked the idea that electrosprayed proteins can retain much of their solution structure. This concept was initially met with scepticism [34]. However, it is now well established that gaseous protein ions can get kinetically trapped in solution-like structures, provided that the experimental conditions are properly optimized [7,35-37].

In native ESI-MS it is essential to minimize structural perturbations of the analyte during its journey from bulk solution into highly charged ESI droplets, and ultimately into the gas phase [16,38]. One parameter that has to be carefully controlled is the extent of collisional heating in the ion sampling interface. Conditions that are too gentle cause

inadequate desolvation, while excess activation disrupts noncovalent contacts and causes gas phase unfolding [39,40]. In addition to these gas phase events, it is necessary to minimize structural perturbations that might take place while the protein is still surrounded by solvent. Examples of such events include thermal denaturation due to inadvertent heating [41,42], as well as surface adsorption within the ESI capillary [43].

### **pH Changes During the ESI Process**

An obvious concern in native ESI-MS is the risk of pH-induced structural perturbations during the analytical workflow. Processes that alter the solution pH can be encountered at various stages (Figure 1). The acid/base milieu of the bulk analyte solution may undergo changes in experiments where native ESI-MS is used for on-line investigations of biomolecular processes [44,45]. This issue deserves particular attention when probing enzymatic reactions that consume or produce pH-active compounds [46-48].

Charge-balancing redox processes within the ESI capillary affect the solution chemistry [49]. Positive ion mode (which is typically used in native ESI-MS) causes acidification due to oxidation reactions such as  $2 \text{H}_2\text{O} \rightarrow 4 \text{H}^+ + 4\text{e}^- + \text{O}_2$  [50]. This effect was strikingly demonstrated by Van Berkel et al. [51] in experiments on nanoESI capillaries containing indicator dyes. For unbuffered solutions those emitters showed pH changes from the near-neutral range to pH 3, under some conditions even down to pH 1.4. Similarly, the operation of an ESI source in negative ion mode increases pH due to reduction processes (e.g.,  $2 \text{H}_2\text{O} + 2\text{e}^- \rightarrow 2 \text{OH}^- + \text{H}_2$ ) [50]. The magnitude of these pH changes depends on the length of time during which the analyte solution is subject to solvent electrolysis [51]. The high surface to volume ratio at the outlet of nanoESI emitters may cause additional pH modulations due to the effects of silanol groups (and/or other titratable sites) on the acid/base chemistry of the analyte solution [52].

Spectroscopic experiments revealed that pH changes can also take place within ESI droplets [53,54]. Initial droplets generated at the Taylor cone have radii  $r$  around 150 to 1500 nm for nanoESI and ESI, respectively [16,55]. Evaporation and fission events produce successively smaller droplets, down to  $r$  values of a few nm. Throughout this process the droplets stay close to the Rayleigh limit, where the number of excess charges is  $z_R = 8\pi(\epsilon_0\gamma^3)^{1/2} / e$  with  $\epsilon_0$  = vacuum permittivity,  $e$  = elementary charge, and  $\gamma = 0.072$  N m<sup>-1</sup> for water at 298 K [16,56]. According to the charged residue model (CRM), analyte ions in native ESI are released as the final nanodroplets evaporate to dryness [9,16,57,58].

One can perform simple back-of-the-envelope calculations to predict how these CRM events might affect the droplet pH. For this purpose we make a few simplifying assumptions. (i) The solution is unbuffered and initially has neutral pH; (ii) contributions of analyte molecules to the droplet volume and solution chemistry are negligible; (iii) the droplets remain at  $z_R$  due to the presence of the charge carriers Na<sup>+</sup>, NH<sub>4</sub><sup>+</sup>, or H<sup>+</sup>. (iv) Charge carriers are homogeneously distributed throughout the droplet. It is clear that these four assumptions do not fully capture all the subtleties associated with the droplet chemistry [16,56,59,60]. For example, some charge carriers may accumulate on the droplet surface [59], while others prefer the interior [38,61] such that a strict definition of droplet pH may not always be straightforward. The assumptions outlined above nonetheless should be adequate for semi-quantitative estimations of an “average” droplet pH. The charge carrier concentration  $C$  can then be approximated as

$$C = \frac{z_R}{N_A \times (\text{droplet volume})} \quad (1)$$

with  $N_A = 6.02 \times 10^{23}$  mol<sup>-1</sup>, such that pH can be estimated as a function of droplet size (Figure 2a). Droplets charged with Na<sup>+</sup> remain neutral because Na<sup>+</sup> is a spectator ion. For

droplets charged with  $\text{NH}_4^+$  the pH decreases with decreasing droplet size, because  $\text{NH}_4^+$  is a weak acid. The possible evaporation of neutral ammonia (a weak base) from the droplet would further enhance this pH decrease. An even more dramatic acidification is predicted for droplets that are charged with protons (Figure 2a, magenta profile). Readers might object that  $\text{H}^+$ -charged droplets are unlikely to form from a neutral pH solution, but we recall that water oxidation provides a steady supply of protons in the ESI capillary (see above) [50].

Overall, the profiles of Figure 2a demonstrate that proteins within the ESI plume can experience significant pH-induced stress, with  $\text{pH} < 1$  during the final stages of solvent evaporation (Figure 2b, c). The predicted pH is lowest when the droplets reach their minimum size, i.e., when the final layers of solvent evaporate and the protein is released. Small proteins will thus experience a more acidic pH than large proteins, illustrated in Figure 1a for ubiquitin ( $r \approx 1$  nm, final  $\text{pH} \approx -0.2$ ) and for pyruvate kinase ( $r \approx 5$  nm, final  $\text{pH} \approx 1$ ).

Admittedly, the pH estimates obtained for the magenta ( $\text{H}^+$ ) profile of Figure 2a represent a worst-case scenario. The actual evolution of droplet pH depends on many factors, including the possible presence of species that mitigate acidification. Also, the net droplet charge will usually be composed of different charge carriers, not just protons. When designing native ESI-MS experiments, one should nonetheless not dismiss the possibility that ESI droplets can undergo significant acidification. These effects are in addition to pH changes that may take place elsewhere in the ESI source (Figure 1).

### **Can Inadvertent pH Changes Affect the Outcome of ESI-MS Experiments?**

It is undisputed that native ESI-MS is a powerful approach for probing protein structures and interactions, evidenced by the successful detection of numerous biomolecular systems in the gas phase [1-15]. Nonetheless, a significant number of studies have reported discrepancies between solution and gas phase behavior. This issue seems to be particularly prevalent for



complexes containing metal ions [62-66]. The underlying reasons are not always clear, but several authors have attributed effects of this kind to ESI-induced pH artifacts, consistent with the processes outlined in Figure 1 [62,63,65,67,68].

Whether or not ESI-induced pH artifacts affect the outcome of MS experiments depends not only on the thermodynamic stability of the analyte, but also on kinetic aspects [69]. Some binding equilibria respond to solvent changes quite slowly, such that pH changes during ESI are masked by the short ( $\mu\text{s}$  -  $\text{ms}$ ) lifetimes of ESI droplets [70,71]. Other systems react sufficiently fast to allow major pH-induced changes during the droplet stage [72,73].

ESI charge state distributions are a widely used tool for monitoring protein conformational changes that take place in bulk solution. These studies rely on the fact that native proteins produce low charge states, while unfolded chains generate ions that are more extensively protonated [38,74-76]. The addition of organic acids is the most common approach for inducing protein unfolding in bulk solution. Denaturation profiles obtained in this way are often in reasonable agreement with solution-phase spectroscopic data [74-76], seemingly indicating that ESI-induced pH changes are not a major issue. However, pH artifacts may be difficult to detect, because unfolding midpoints measured by ESI-MS can be skewed by differences in the detection efficiency of folded vs. unfolded proteins [38]. In addition, the logarithmic nature of the pH axis, along with the fact that many proteins unfold below pH 3, tends to be somewhat deceiving. This can be illustrated by considering a bulk solution that contains 1 mM  $\text{H}^+$ , corresponding to pH 3. Doubling the  $\text{H}^+$  concentration to 2 mM (e.g., as the result of water hydrolysis during ESI [51]) will lower the pH to 2.7. Such a relatively small pH shift may easily be overlooked. ESI-induced pH artifacts are more apparent for proteins that start to unfold around pH 5 - 6. In such cases it is not uncommon to observe charge state distributions that are inconsistent with bulk solution data, implying that ESI-mediated acidification has affected the protein structure [77,78]. In summary, there is

clear evidence that inadvertent pH changes can take place during ESI, and that this phenomenon can influence the outcome of ESI-MS experiments in undesired ways.

## Buffers

The use of a buffer is an obvious strategy for stabilizing the pH throughout the various stages of the ESI process (Figure 1). By definition, a buffer is a mixture of a weak acid and its conjugate weak base. Both components have to be present in appreciable concentrations. The buffering range comprises the weak acid  $pK_a \pm 1$  pH unit, and the buffer pH is governed by the Henderson–Hasselbalch equation [26,79]

$$pH = pK_a + \log \frac{[\textit{conjugate base}]}{[\textit{conjugate acid}]} \quad (2)$$

For choosing an appropriate buffer one has to select a system with an acid  $pK_a$  that is close to the desired pH value. For physiological samples  $pK_a \approx 7$  is desirable. Phosphate buffer is widely used for bulk solution studies because  $H_2PO_4^-$  has a  $pK_a$  of 7.2. Its conjugate base is  $HPO_4^{2-}$ . From equation 2 it can be determined that a neutral 10 mM sodium phosphate buffer contains 3.9 mM  $Na_2HPO_4$  and 6.1 mM  $NaH_2PO_4$ . When 1 mM  $H^+$  are added to this buffer (corresponding to water oxidation under typical nanoESI conditions [51]), the buffer will respond with a slight acidification to pH 6.8.

Next, we consider a buffer system that is not well suited for the neutral range. Acetic acid and acetate are a conjugate weak acid/base pair with  $pK_a = 4.75$ . A 10 mM pH 7 acetate “buffer” contains 9.943 mM acetate and 0.057 mM acetic acid. The addition of 1 mM  $H^+$  decreases the pH to 5.8. This large drop reflects the fact that the initial pH is not within the

buffering range of  $pK_a \pm 1$  pH unit. For comparison, a drop down to pH 3 would take place in pure water.

Unfortunately, phosphate solutions and most other buffer systems commonly used in biochemistry laboratories are non-volatile and therefore incompatible with ESI-MS [80]. Major interferences arise from the fact that cationic and anionic components (such as  $Na^+$ ,  $H_2PO_4^-$  and  $HPO_4^{2-}$ ) form nonspecific adducts with analytes during ESI [16,81]. The situation is different for ammonium and acetate, both of which are volatile. Like other electrolytes, they form nonspecific adducts with the analyte during the final stages of ESI. However, protonation of acetate in positive ion mode generates acetic acid which dissociates in the declustering region of the mass spectrometer. Similarly,  $NH_4^+$  adducts release  $NH_3$  and leave behind a proton, thereby favoring the formation of clean  $[M + zH]^{z+}$  ions [16,80]. This volatility makes ammonium acetate an electrospray-friendly additive that is widely used in native ESI-MS, often at concentrations around 10 mM [4,12,15,16,32,82-86].

ESI-MS can readily deal with non-volatile additives as long as on-line liquid chromatography or other sample clean-up steps are incorporated into the workflow. However, the current discussion focuses on native ESI-MS which is much more unforgiving because analyte solution is sprayed directly into the ion sampling interface of the mass spectrometer.

### **Is Ammonium Acetate a Buffer at Neutral pH?**

Numerous papers have repeated the claim that neutral ammonium acetate solutions are “buffered”. This habit is commonplace in ESI-MS publications, although it predates the inception of electrospray by several decades [87]. The term “ammonium acetate buffer” implies a sense of security, suggesting that biomolecular analytes will be protected from pH-induced degradation throughout the ESI process (Figure 1). Sadly, the designation of ammonium acetate as a neutral buffer is misleading.

Ammonium is a weak acid, and acetate is a weak base. It is a quirk of nature that the acidity of  $\text{NH}_4^+$  ( $\text{pK}_a$  9.25) exactly balances the basicity of acetate ( $\text{pK}_b$  9.25), such that dissolution of ammonium acetate salt in pure water produces a neutral pH solution [87,88]. Perhaps it is this peculiar feature that has caused many practitioners to misjudge the properties of ammonium acetate.

Ammonium and acetate are *not* a conjugate acid/base pair. The two species are *not* related via a single ( $\text{HA} \leftrightarrow \text{H}^+ + \text{A}^-$  or  $\text{HA}^+ \leftrightarrow \text{H}^+ + \text{A}$ ) equilibrium that would be required for the validity of equation 2. A proper buffer has its  $\text{pK}_a$  within  $\pm 1$  unit of the desired pH [79]. Neither ammonium/ammonia ( $\text{pK}_a$  9.25) nor acetic acid/acetate ( $\text{pK}_a$  4.75) meet this criterion for pH 7. By definition, therefore, *ammonium acetate is not a buffer at pH 7*. This simple fact has been largely ignored in the ESI-MS literature, except for rare cautionary remarks that are easily overlooked [16].

Despite this negative verdict, the acid/base chemistry of ammonium acetate can be put to good use in native ESI-MS. Sub-stoichiometric acidification converts a certain percentage of acetate to acetic acid. These conditions produce an acetate buffer that stabilizes the pH at  $4.75 \pm 1$ . The properties of acetate buffers have been discussed in the previous section, where we noted that addition of 1 mM  $\text{H}^+$  to a 10 mM neutral pH solution will decrease the pH to 5.8. This is less dramatic than the drop to pH 3 that would occur in pure water. Thus, ammonium acetate *does* have a pH buffering effect in the acidic range, but this effect is not felt until the solution is within roughly  $\pm 1$  pH unit of the acetic acid  $\text{pK}_a$  (4.75). There are only a few instances in the ESI-MS literature where ammonium acetate was correctly referred to as a pH 5 buffer [33,72].

Alkalinization of ammonium acetate solution generates  $\text{NH}_3$  via de-protonation of  $\text{NH}_4^+$ , thereby generating a buffer around the  $\text{pK}_a$  of ammonium (9.25). Thus, ammonium

acetate also buffers pH in the basic range, but this effect is insignificant until the solution is within  $\pm 1$  pH unit of the ammonium  $pK_a$ .

The concepts outlined above are easily verified by generating experimental titration profiles (Figure 3). Regions that lack buffering capacity are characterized by steep slopes. Buffered regions have shallow slopes, implying that the addition of  $H^+$  or  $OH^-$  alters pH only slightly. As expected, dramatic pH changes are seen in pure water which has no buffering capacity (Figure 3a). Excellent pH stabilization in the neutral pH range is obtained when using a phosphate buffer (Figure 3b). Ammonium acetate does not buffer around pH 7, but it stabilizes the pH in the range of  $4.75 \pm 1$  and  $9.25 \pm 1$ . These two regions reflect buffering by  $CH_3-COOH/CH_3-COO^-$  and  $NH_4^+/NH_3$ , respectively (Figure 3c) [89].

### **Should Practitioners Continue to Use Ammonium Acetate?**

Ammonium acetate has a number of attractive features that make it a useful additive in native ESI-MS, as long as practitioners are aware of the limitations. While ammonium acetate is not a buffer at pH 7, it still exerts a moderating effect on pH alterations encountered during ESI. In positive ion mode there are several factors that tend to acidify the analyte solution (Figure 1). Ammonium acetate mitigates these effects by buffering the solution in the range of  $4.75 \pm 1$ . Hence, an initially neutral ammonium acetate solution should be expected to have a pH of  $4.75 \pm 1$  at the point of analyte release in positive ion mode. This acidification is severe enough to cause the protonation of His ( $pK_a \sim 7$ ), but it will leave Asp and Glu carboxylates ( $pK_a \sim 4$ ) largely unaffected. Analogously, in negative ion ESI the electrolytic production of  $OH^-$  tends to increase pH. Ammonium acetate will cap this alkalization at pH  $9.25 \pm 1$ . Under these condition Lys ( $pK_a \sim 11$ ) and Arg ( $pK_a \sim 12$ ) will retain their canonical positive charge.

At any rate, the use of ammonium acetate solutions in native ESI-MS is preferable over pure water. Pure water may result in extreme acidification during the final stages of droplet shrinkage (Figure 2a, magenta). Acetate buffering will lessen this acidification by ensuring that the pH does not drop below  $4.75 \pm 1$ . This behavior is consistent with experimental observations, e.g., apomyoglobin in pure water produces high ESI charge states that indicate acid-induced unfolding. In ammonium acetate solution the spectrum shifts to lower charge states, implying the prevalence of compact structures (Fig. 3 in ref. [78]).

Although many native ESI-MS studies have employed ammonium acetate at concentrations around 10 mM [4,12,15,16,32,82-86], higher concentrations can often be tolerated [1,5,7,8,11,40,86]. These higher concentrations may help mitigate pH changes during the ESI process. As noted, the addition of 1 mM  $H^+$  (e.g., from water oxidation [51]) will lower the pH of a 10 mM ammonium acetate solution from pH 7 to 5.8. For a 100 mM solution the pH will only drop to 6.5 under otherwise identical conditions. However, the increased electrolyte concentration will enhance the rate of electrochemical processes within the ESI source, such that the  $H^+$  production is expected to rise when more ammonium acetate is added [16]. Also, the volatile nature of ammonium acetate makes it difficult to predict in how far elevated concentrations would help suppress pH changes within ESI droplets (Figure 2a).

Ammonium acetate possesses additional attributes that contribute to its popularity in ESI-MS. Biomolecular structures and interactions in solution depend on the presence of dissolved salts [86,90-92]. Classical electrolytes (NaCl, KCl, etc.) are non-volatile and cause interferences [16,81]. Due to its volatile nature, ammonium acetate does not degrade the spectral quality, offering mass spectrometrists the opportunity to work in an ionic milieu that is acceptable to classically trained biochemists. As an added bonus, ammonium acetate can

even suppress the formation of undesired salt adducts by competing with non-volatile electrolytes for binding sites at the protein surface [80].

### **Other ESI-Friendly Solvent Additives and Buffers**

The number of ESI-compatible (volatile) additives that buffer in the neutral range is limited. This may be the main reasons why ammonium acetate has become the *de facto* standard for native ESI-MS. Ammonium bicarbonate represents an interesting option, considering that  $\text{HCO}_3^-$  has a  $\text{pK}_a$  of 6.4 which is a reasonable match for pH 7 solutions [88]. Unfortunately, ammonium bicarbonate tends to induce protein unfolding during ESI. This phenomenon has been attributed to protein interactions with bubbles formed by  $\text{CO}_2$  outgassing at the droplet stage [89], possibly in combination with other factors [93]. Because of this destabilizing effect, it would be prudent to avoid ammonium bicarbonate in native ESI-MS [89]. Ammonium formate is another volatile salt, but it is even less suitable for neutral pH buffering than ammonium acetate due to the  $\text{pK}_a$  of formic acid/formate (3.75) [88]. Various alkyl-ammonium acetate salts have been used for mechanistic investigations [81,94], but they also do not provide buffering at neutral pH based on the  $\text{pK}_a$  values involved.

The term “buffer” may also be used in different contexts. Redox buffers stabilize the interfacial potential within the ESI source. Examples of such substances include ascorbic acid and easily oxidizable metals [95,96]. Redox buffers can reduce pH changes in the ESI source by suppressing water electrolysis. However, we will not discuss this aspect in greater detail because our focus is on classical acid/base buffering. Readers interested in ESI-related redox chemistry can refer to recent reviews [49,50].

## Conclusions

Undergraduate chemistry students are taught that a buffer provides pH stabilization in a range of the weak acid  $pK_a \pm 1$  pH unit [79]. For pH 7, ammonium acetate does not match this criterion. Both of the relevant  $pK_a$  values (4.75 for acetic acid and 9.25 for ammonia) are 2.25 units away from the desired neutral pH. It is true that dissolution of ammonium acetate salt in pure water produces a neutral pH solution. However, this solution is not buffered, and it will undergo significant pH changes upon addition of small amounts of  $H^+$  or  $OH^-$ .

Aqueous ammonium acetate solution at pH 7 remains a useful solvent for native ESI-MS, as long as practitioners are aware of its limitations. Protein stability is often reduced in the absence of dissolved salts, and ammonium acetate can serve as a stabilizing background electrolyte. Positive ion mode ESI tends to result in acidification of the analyte solution. In the presence of ammonium acetate the pH may drop to values as low as  $4.75 \pm 1$  in the final ESI droplets, reflecting the  $pK_a$  of acetate buffer. Conversely, experiments in negative ion mode likely result in final pH values around  $9.25 \pm 1$  as a result of  $NH_4^+/NH_3$  buffering.

It is hoped that this Critical Insight article will dispel some of the myths surrounding the properties of ammonium acetate. Practitioners should avoid the term “ammonium acetate buffer” when referring to neutral conditions, as this wording choice is highly misleading. The term “ammonium acetate *buffer*” is only justified if the pH is around 4.75 or 9.25. In all other cases (specifically around pH 7) “ammonium acetate *solution*” should be used. This change in terminology will help avoid false expectations regarding the acid/base environment of analytes under ESI conditions. It is hoped that future work will yield improved approaches for dealing with physiologically relevant buffer systems in ESI-MS. Interesting recent developments in this area include the use of nanoESI emitters with  $\mu m$  outlet diameter [29], as well as fused-droplet ESI [97].



**Acknowledgments.** Funding for this work was provided by the Natural Sciences and Engineering Research Council of Canada (Discovery Grant 217080-2013). Victor Yin and Yiming Xiao are acknowledged for critical reading of the manuscript.

## References

1. Leney, A.C., Heck, A.J.R.: Native Mass Spectrometry: What is in the Name? *J. Am. Soc. Mass Spectrom.* **28**, 5-13 (2017)
2. Fatunmbi, O., Abzalimov, R.R., Savinov, S.N., Gershenson, A., Kaltashov, I.A.: Interactions of Haptoglobin with Monomeric Globin Species: Insights from Molecular Modeling and Native Electrospray Ionization Mass Spectrometry. *Biochemistry* **55**, 1918-1928 (2016)
3. Konijnenberg, A., Butterer, A., Sobott, F.: Native ion mobility-mass spectrometry and related methods in structural biology. *Biochim. Biophys. Acta* **1834**, 1239-1256 (2013)
4. Ashcroft, A.E.: Mass Spectrometry and the Amyloid Problem - How Far Can We Go in the Gas Phase? *J. Am. Soc. Mass Spectrom.* **21**, 1087-1096 (2010)
5. Landreh, M., Marklund, E.G., Uzdavinys, P., Degiacomi, M.T., Coincon, M., Gault, J., Gupta, K., Liko, I., Benesch, J.L.P., Drew, D., Robinson, C.V.: Integrating mass spectrometry with MD simulations reveals the role of lipids in Na<sup>+</sup>/H<sup>+</sup> antiporters. *Nat. Commun.* **8** (2017)
6. Dyachenko, A., Gruber, R., Shimon, L., Horovitz, A., Sharon, M.: Allosteric mechanisms can be distinguished using structural mass spectrometry. *Proc. Natl. Acad. Sci. U. S. A.* **110**, 7235-7239 (2013)
7. Deng, L., Broom, A., Kitova, E.N., Richards, M.R., Zheng, R.B., Shoemaker, G.K., Meiering, E.M., Klassen, J.S.: Kinetic Stability of the Streptavidin-Biotin Interaction Enhanced in the Gas Phase. *J. Am. Chem. Soc.* **134**, 16586-16596 (2012)
8. Zhang, H., Cui, W., Gross, M.L.: Native electrospray ionization and electron-capture dissociation for comparison of protein structure in solution and the gas phase. *Int. J. Mass Spectrom.* **354-355**, 288-291 (2013)
9. Porrini, M., Rosu, F., Rabin, C., Darre, L., Gomez, H., Orozco, M., Gabelica, V.: Compaction of Duplex Nucleic Acids upon Native Electrospray Mass Spectrometry. *ACS Central Sci.* **3**, 454-461 (2017)
10. Shelimov, K.B., Clemmer, D.E., Hudgins, R.R., Jarrold, M.F.: Protein Structure in Vacuo: The Gas-Phase Conformation of BPTI and Cytochrome c. *J. Am. Chem. Soc.* **119**, 2240-2248 (1997)

11. Chen, S.-H., Russell, D.H.: How Closely Related Are Conformations of Protein Ions Sampled by IM-MS to Native Solution Structures? *J. Am. Soc. Mass Spectrom.* **26**, 1433-1443 (2015)
12. Ruotolo, B.T., Hyung, S.-J., Robinson, P.M., Giles, K., Bateman, R.H., Robinson, C.V.: Ion Mobility–Mass Spectrometry Reveals Long-Lived, Unfolded Intermediates in the Dissociation of Protein Complexes. *Angew. Chem. Int. Ed.* **46**, 8001-8004 (2007)
13. Wyttenbach, T., Bleiholder, C., Bowers, M.T.: Factors contributing to the collision cross section of polyatomic ions in the kilodalton to gigadalton range: application to ion mobility measurements. *Anal. Chem.* **85**, 2191-2199 (2013)
14. Kaddis, C.S., Loo, J.A.: Native Protein MS and Ion Mobility: Large Flying Proteins with ESI. *Anal. Chem.* **79**, 1779-1784 (2007)
15. Jurneczko, E., Barran, P.E.: How useful is ion mobility mass spectrometry for structural biology? The relationship between protein crystal structures and their collision cross sections in the gas phase. *Analyst* **136**, 20-28 (2011)
16. Kebarle, P., Verkerk, U.H.: Electrospray: From Ions in Solutions to Ions in the Gas Phase, What We Know Now. *Mass Spectrom. Rev.* **28**, 898-917 (2009)
17. Fersht, A.R. *Structure and Mechanism in Protein Science*; W. H. Freeman & Co.: New York, 1999.
18. Southall, N.T., Dill, K.A., Haymett, A.D.J.: A View of the Hydrophobic Effect. *J. Phys. Chem. B* **106**, 521-533 (2002)
19. Grdadolnik, J., Merzel, F., Avbelj, F.: Origin of hydrophobicity and enhanced water hydrogen bond strength near purely hydrophobic solutes. *Proc. Natl. Acad. Sci. U. S. A.* **114**, 322-327 (2017)
20. Ball, P.: Water as an Active Constituent in Cell Biology. *Chem. Rev.* **108**, 74-108 (2008)
21. Kumar, S., Nussinov, R.: Salt bridge stability in monomeric proteins. *J. Mol. Biol.* **293**, 1241-1255 (1999)
22. Kunz, W., Lo Nostro, P., Ninham, B.W.: The present state of affairs with Hofmeister effects. *Curr. Opin. Colloid Interface Sci.* **9**, 1-18 (2004)

23. Creighton, T.E. *Proteins*; W. H. Freeman & Co: New York, 1993.
24. Deutsch, C., Taylor, J.S., Wilson, D.F.: Regulation of intracellular pH by human peripheral blood lymphocytes as measured by <sup>19</sup>F NMR. *Proc. Natl. Acad. Sci. U. S. A.* **79**, 7944-7948 (1982)
25. Boron, W.F.: Regulation of intracellular pH. *Adv. Physiol. Educ.* **28**, 160-179 (2004)
26. Nielsen, J.E. Analyzing enzymatic pH activity profiles and protein titration curves using structure-based pKa calculations and titration curve fitting. In *Meth. Enzymol.*; Johnson, M. L.; Brand, L. Eds.; Elsevier Academic Press Inc: San Diego, 2009; Vol. 454; pp. 233-258.
27. Bisswanger, H.: Enzyme assays. *Perpect. Sci.* **1**, 41-55 (2014)
28. Bramaud, C., Aimar, P., Daufin, G.: Thermal isoelectric precipitation of alpha-lactalbumin from a whey protein concentrate: Influence of protein-calcium complexation. *Biotechnol. Bioeng.* **47**, 121-130 (1995)
29. Susa, A.C., Xia, Z.J., Williams, E.R.: Small Emitter Tips for Native Mass Spectrometry of Proteins and Protein Complexes from Nonvolatile Buffers That Mimic the Intracellular Environment. *Anal. Chem.* **89**, 3116-3122 (2017)
30. Fenn, J.B., Mann, M., Meng, C.K., Wong, S.F., Whitehouse, C.M.: Electrospray Ionization for Mass Spectrometry of Large Biomolecules. *Science* **246**, 64-71 (1989)
31. Katta, V., Chait, B.T.: Observation of the Heme-Globin Complex in Native Myoglobin by Electrospray-Ionisation Mass Spectrometry. *J. Am. Chem. Soc.* **113**, 8534-8535 (1991)
32. Light-Wahl, K.J., Schwartz, B.L., Smith, R.D.: Observation of the Noncovalent Quaternary Association of Proteins by Electrospray Ionization Mass Spectrometry. *J. Am. Chem. Soc.* **116**, 5271-5278 (1994)
33. Ganem, B., Li, Y.-T., Henion, J.D.: Observation of Noncovalent Enzyme-Substrate and Enzyme-Product Complexes by Ion-Spray Mass Spectrometry. *J. Am. Chem. Soc.* **113**, 7818-7819 (1991)

34. Wolynes, P.G.: Biomolecular folding in vacuo!!!(?). *Proc. Natl. Acad. Sci. U.S.A.* **92**, 2426-2427 (1995)
35. Hendricks, N.G., Julian, R.R.: Leveraging ultraviolet photodissociation and spectroscopy to investigate peptide and protein three-dimensional structure with mass spectrometry. *Analyst* **141**, 4534-4540 (2016)
36. Silveira, J.A., Fort, K.L., Kim, D., Servage, K.A., Pierson, N.A., Clemmer, D.E., Russell, D.H.: From Solution to the Gas Phase: Stepwise Dehydration and Kinetic Trapping of Substance P Reveals the Origin of Peptide Conformations. *J. Am. Chem. Soc.* **135**, 19147-19153 (2013)
37. Hamdy, O.M., Julian, R.R.: Reflections on Charge State Distributions, Protein Structure, and the Mystical Mechanism of Electrospray Ionization. *J. Am. Soc. Mass Spectrom.* **23**, 1-6 (2012)
38. Konermann, L., Ahadi, E., Rodriguez, A.D., Vahidi, S.: Unraveling the Mechanism of Electrospray Ionization. *Anal. Chem.* **85**, 2-9 (2013)
39. Clemmer, D.E., Jarrold, M.F.: Ion Mobility Measurements and their Applications to Clusters and Biomolecules. *J. Mass Spectrom.* **32**, 577-592 (1997)
40. Benesch, J.L.P., Ruotolo, B.T., Simmons, D.A., Robinson, C.V.: Protein Complexes in the Gas Phase: Technology for Structural Genomics and Proteomics. *Chem. Rev.* **107**, 3544-3567 (2007)
41. Mirza, U.A., Chait, B.T.: Do proteins denature during droplet evolution in electrospray ionization. *Int. J. Mass. Spectrom. Ion Proc.* **162**, 173-181 (1997)
42. Kitova, E.N., El-Hawiet, A., Schnier, P.D., Klassen, J.S.: Reliable Determinations of Protein-Ligand Interactions by Direct ESI-MS Measurements. Are We There Yet? *J. Am. Soc. Mass Spectrom.* **23**, 431-441 (2012)
43. Mortensen, D.N., Williams, E.R.: Surface-Induced Protein Unfolding in Submicron Electrospray Emitters. *Anal. Chem.* **88**, 9662-9668 (2016)
44. Debaene, F., Wagner-Rousset, E., Colas, O., Ayoub, D., Corvaia, N., Van Dorsselaer, A., Beck, A.H., Cianférani, S.: Time Resolved Native Ion-Mobility Mass Spectrometry to Monitor Dynamics of IgG4 Fab Arm Exchange and “Bispecific” Monoclonal Antibody Formation. *Anal. Chem.* **85**, 9785-9792 (2013)

45. Fändrich, M., Tito, M.A., Leroux, M.R., Rostom, A.A., Hartl, F.U., Dobson, C.M., Robinson, C.V.: Observation of the noncovalent assembly and disassembly pathways of the chaperone complex MtGimC by mass spectrometry. *Proc. Natl. Acad. Sci. U.S.A.* **97**, 14151-14155 (2000)
46. Liuni, P., Jeganathan, A., Wilson, D.J.: Conformer Selection and Intensified Dynamics During Catalytic Turnover in Chymotrypsin. *Angew. Chem. Int. Ed.* **51**, 9666 – 9669 (2012)
47. Li, Z., Sau, A.K., Shen, S., Whitehouse, C., Baasov, T., Anderson, K.S.: A snapshot of Enzyme Catalysis Using Electrospray Mass Spectrometry. *J. Am. Chem. Soc.* **125**, 9938-9939 (2003)
48. Chen, Y.C., Urban, P.L.: Time-resolved mass spectrometry. *Trac-Trends Anal. Chem.* **44**, 106-120 (2013)
49. Pozniak, B.P., Cole, R.B.: Perspective on Electrospray Ionization and Its Relation to Electrochemistry. *J. Am. Soc. Mass Spectrom.* **26**, 369-385 (2015)
50. Van Berkel, G.J., Kertesz, V.: Using the Electrochemistry of the Electrospray Ion Source. *Anal. Chem.* **79**, 5511-5520 (2007)
51. Van Berkel, G.J., Asano, K.G., Schnier, P.D.: Electrochemical Processes in a Wire-in-a-Capillary Bulk-Loaded, Nano-Electrospray Emitter. *J. Am. Soc. Mass Spectrom.* **12**, 853-862 (2001)
52. Horvath, J., Dolnik, V.: Polymer wall coatings for capillary electrophoresis. *Electrophoresis* **22**, 644-655 (2001)
53. Zhou, S., Prebyl, B.S., Cook, K.D.: Profiling pH Changes in the Electrospray Plume. *Anal. Chem.* **74**, 4885-4888 (2002)
54. Girod, M., Dagany, X., Antoine, R., Dugourd, P.: Relation between charge state distributions of peptide anions and pH changes in the electrospray plume. A mass spectrometry and optical spectroscopy investigation. *Int. J. Mass Spectrom.* **308**, 41-48 (2011)
55. Kebarle, P., Tang, L.: From ions in solution to ions in the gas phase: The mechanism of electrospray mass spectrometry. *Anal. Chem.* **65**, 972A-986A (1993)

56. Smith, J.N., Flagan, R.C., Beauchamp, J.L.: Droplet Evaporation and Discharge Dynamics in Electrospray Ionization. *J. Phys. Chem. A* **106**, 9957-9967 (2002)
57. de la Mora, F.J.: Electrospray Ionization of large multiply charged species proceeds via Dole's charged residue mechanism. *Anal. Chim. Acta* **406**, 93-104 (2000)
58. McAllister, R.G., Metwally, H., Sun, Y., Konermann, L.: Release of Native-Like Gaseous Proteins from Electrospray Droplets via The Charged Residue Mechanism: Insights from Molecular Dynamics Simulations. *J. Am. Chem. Soc.* **137**, 12667-12676 (2015)
59. Iyengar, S.S., Day, T.J.F., Voth, G.A.: On the amphiphilic behavior of the hydrated proton: an ab initio molecular dynamics study. *Int. J. Mass Spectrom.* **241**, 197-204 (2005)
60. Lee, J.W., Kim, H.I.: Investigating acid-induced structural transitions of lysozyme in an electrospray ionization source. *Analyst* **140**, 661-669 (2015)
61. Znamenskiy, V., Marginean, I., Vertes, A.: Solvated Ion Evaporation from Charged Water Droplets. *J. Phys. Chem. A* **107**, 7406-7412 (2003)
62. McDonald, L.W., Campbell, J.A., Clark, S.B.: Failure of ESI Spectra to Represent Metal-Complex Solution Composition: A Study of Lanthanide-Carboxylate Complexes. *Anal. Chem.* **86**, 1023-1029 (2014)
63. Wang, H., Agnes, G.R.: Kinetically Labile Equilibrium Shifts Induced by the Electrospray Process. *Anal. Chem.* **71**, 4166-4172 (1999)
64. Zhang, M.X., Gumerov, D.R., Kaltashov, I.A., Mason, A.B.: Indirect detection of protein-metal binding: Interaction of serum transferrin with  $\text{In}^{3+}$  and  $\text{Bi}^{3+}$ . *J. Am. Soc. Mass Spectrom.* **15**, 1658-1664 (2004)
65. Bich, C., Baer, S., Jecklin, M.C., Zenobi, R.: Probing the Hydrophobic Effect of Noncovalent Complexes by Mass Spectrometry. *J. Am. Soc. Mass Spectrom.* **21**, 286-289 (2010)
66. Jecklin, M.C., Touboul, D., Bovet, C., Wortmann, A., Zenobi, R.: Which Electrospray-Based Ionization Method Best Reflects Protein-Ligand Interactions Found in Solution? A Comparison of ESI, nanoESI, and ESSI for the Determination of Dissociation Constants with Mass Spectrometry. *J. Am. Soc. Mass Spectrom.* **19**, 332-343 (2008)

67. Wang, W., Kitova, E.N., Klassen, J.S.: Influence of solution and gas phase processes on protein-carbohydrate binding affinities determined by nanoelectrospray Fourier transform ion cyclotron resonance mass spectrometry. *Anal. Chem.* **75**, 4945-4955 (2003)
68. Liang, Y., Du, F., Sanglier, S., Zhou, B.R., Xia, Y., Van Dorsselaer, A., Maechling, C., Kilhoffer, M.C., Haiech, J.: Unfolding of rabbit muscle creatine kinase induced by acid - A study using electrospray ionization mass spectrometry, isothermal titration calorimetry, and fluorescence spectroscopy. *J. Biol. Chem.* **278**, 30098-30105 (2003)
69. Di Marco, V.B., Bombi, G.G.: Electrospray mass spectrometry (ESI-MS) in the study of metal-ligand solution equilibria. *Mass Spec. Rev.* **25**, 347-379 (2006)
70. Wortmann, A., Kistler-Momotova, A., Zenobi, R., Heine, M.C., Wilhelm, O., Pratsinis, S.E.: Shrinking Droplets in Electrospray Ionization and Their Influence on Chemical Equilibria. *J. Am. Soc. Mass Spectrom.* **18**, 385-393 (2007)
71. Peschke, M., Verkerk, U.H., Kebarle, P.: Features of the ESI Mechanism that Affect the Observation of Multiply Charged Noncovalent Protein Complexes and the Determination of the Association Constant by the Titration Method. *J. Am. Soc. Mass Spectrom.* **15**, 1424-1434 (2004)
72. Kharlamova, A., Prentice, B.M., Huang, T.-Y., McLuckey, S.A.: Electrospray Droplet Exposure to Gaseous Acids for the Manipulation of Protein Charge State Distributions. *Anal. Chem.* **82**, 7422-7429 (2010)
73. Oh, M.I., Consta, S.: Stability of a Transient Protein Complex in a Charged Aqueous Droplet with Variable pH. *J. Phys. Chem. Lett.* **8**, 80-85 (2017)
74. Borysic, A.J.H., Radford, S.E., Ashcroft, A.E.: Co-populated Conformational Ensembles of b2-Microglobulin Uncovered Quantitatively by Electrospray Ionization Mass Spectrometry. *J. Biol. Chem.* **279**, 27069-27077 (2004)
75. Grandori, R.: Detecting equilibrium cytochrome *c* folding intermediates by electrospray ionization mass spectrometry: Two partially folded forms populate the molten globule state. *Protein Sci.* **11**, 453-458 (2002)
76. Dobo, A., Kaltashov, I.A.: Detection of Multiple Protein Conformational Ensembles in Solution via Deconvolution of Charge-State Distributions in ESI MS. *Anal. Chem.* **73**, 4763-4773 (2001)



77. Konermann, L., Silva, E.A., Sogbein, O.F.: Electrochemically Induced pH Changes Resulting in Protein Unfolding in the Ion Source of an Electrospray Mass Spectrometer. *Anal. Chem.* **73**, 4836-4844 (2001)
78. Wang, F., Tang, X.: Conformational Heterogeneity and Stability of Apomyoglobin Studied by Hydrogen/Deuterium Exchange and Electrospray Ionization Mass Spectrometry. *Biochemistry* **35**, 4069-4078 (1996)
79. Masterton, W.L., Hurley, C.N. *Chemistry, Principles and Reactions* 6th ed.; Brooks/Cole Cengage Learning, 2009.
80. Iavarone, A.T., Udekwu, O.A., Williams, E.R.: Buffer Loading for Counteracting Metal Salt-Induced Signal Suppression in Electrospray Ionization. *Anal. Chem.* **76**, 3944-3950 (2004)
81. Metwally, H., McAllister, R.G., Konermann, L.: Exploring the mechanism of salt-induced signal suppression in protein electrospray mass spectrometry using experiments and molecular dynamics simulations. *Anal. Chem.* **87**, 2434-42 (2015)
82. Griffith, W.P., Kaltashov, I.A.: Protein Conformational Heterogeneity as a Binding Catalyst: ESI-MS Study of Hemoglobin H Formation. *Biochemistry* **46**, 2020-2026 (2007)
83. Apostol, I.: Assessing the relative stabilities of engineered hemoglobins using electrospray mass spectrometry. *Anal. Biochem.* **272**, 8 - 18 (1999)
84. Kang, Y., Douglas, D.J.: Gas-Phase Ions of Human Hemoglobin A, F, and S. *J. Am. Soc. Mass Spectrom.* **22**, 1187-1196 (2011)
85. Scarff, C.A., Patel, V.J., Thalassinou, K., Scrivens, J.H.: Probing Hemoglobin Structure by Means of Traveling-Wave Ion Mobility Mass Spectrometry. *J. Am. Soc. Mass Spectrom.* **20**, 625-631 (2009)
86. Gavriilidou, A.F.M., Gulbakan, B., Zenobi, R.: Influence of Ammonium Acetate Concentration on Receptor Ligand Binding Affinities Measured by Native Nano ESI-MS: A Systematic Study. *Anal. Chem.* **87**, 10378-10384 (2015)
87. Williams, R.J., Lyman, C.M.: A Neutral Buffered Standard for Hydrogen Ion Work and Accurate Titrations Which Can be Prepared in One Minute. *J. Am. Chem. Soc.* **54**, 1911-1912 (1932)

88. Lide, D.R. *CRC Handbook of Chemistry and Physics* 82nd ed.; CRC Press: Boca Raton, London, New York, Washington, 2001.
89. Hedges, J.B., Vahidi, S., Yue, X., Konermann, L.: Effects of Ammonium Bicarbonate on the Electrospray Mass Spectra of Proteins: Evidence for Bubble-Induced Unfolding. *Anal. Chem.* **85**, 6469-6476 (2013)
90. Susa, A.C., Mortenson, D.N., Williams, E.R.: Effects of Cations on Protein and Peptide Charging in Electrospray Ionization from Aqueous Solutions. *J. Am. Soc. Mass Spectrom.* **25**, 918-927 (2014)
91. Wong, M., Khirich, G., Loria, J.P.: What's in Your Buffer? Solute Altered Millisecond Motions Detected by Solution NMR. *Biochemistry* **52**, 6548-6558 (2013)
92. Long, D., Yang, D.: Buffer Interference with Protein Dynamics: A Case Study on Human Liver Fatty Acid Binding Protein. *Biophys. J.* **96**, 1482-1488 (2009)
93. Cassou, C.A., Williams, E.R.: Anions in Electrothermal Supercharging of Proteins with Electrospray Ionization Follow a Reverse Hofmeister Series. *Anal. Chem.* **86**, 1640-1647 (2014)
94. Zhuang, X., Gavriilidou, A.F.M., Zenobi, R.: Influence of Alkylammonium Acetate Buffers on Protein-Ligand Noncovalent Interactions Using Native Mass Spectrometry. *J. Am. Soc. Mass Spectrom.* **28**, 341-346 (2017)
95. Plattner, S., Erb, R., Chervet, J., Oberacher, H.: Ascorbic acid for homogenous redox buffering in electrospray ionization-mass spectrometry. *Anal. Bioanal. Chem.* **404**, 1571-1579 (2012)
96. Van Berkel, G., Kertesz, V.: Redox buffering in an electrospray ion source using a copper capillary emitter. *J. Mass Spectrom.* **36**, 1125-1132 (2001)
97. Shieh, I.-F., Lee, C.-Y., Shiea, J.: Eliminating the Interferences from TRIS Buffer and SDS in Protein Analysis by Fused-Droplet Electrospray Ionization Mass Spectrometry. *J. Proteome Res.* **4**, 606-612 (2005)

## Figure Captions

**Figure 1.** Schematic depiction of an ESI source operated in positive ion mode. Alterations of the solution pH may be caused by (1) bulk solution reactions, (2) charge-balancing redox processes at metal/liquid interfaces, (3) shrinkage of highly charged droplets.

**Figure 2.** Estimated pH values in shrinking aqueous ESI droplets without buffering. (a) pH in Rayleigh-charged droplets vs. droplet radius  $r$ . The profiles are for a droplet charge composed of  $\text{Na}^+$ ,  $\text{NH}_4^+$ , or  $\text{H}^+$ . Values for  $\text{NH}_4^+$  were calculated based on a weak acid dissociation equilibrium with  $\text{pK}_a = 9.25$ . Dashed lines indicate approximate radii of ubiquitin (Ubq, 8.6 kDa) and pyruvate kinase (PK, 230 kDa). (b) and (c) illustrate droplets where the entire Rayleigh charge is due to protons, representing intermediate stages of a protein CRM process. The pdb file used is 1wla (myoglobin).

**Figure 3.** Experimentally determined titration curves. (a) Pure water, (b) 25 mM sodium phosphate in water, (c) 25 mM ammonium acetate in water. Hatch marks indicate the range where the solutions are buffered (weak acid  $\text{pK}_a \pm 1$  pH unit). For panel (b):  $\text{pK}_a(\text{H}_2\text{PO}_4^-) = 7.2$ . For panel (c):  $\text{pK}_a(\text{acetic acid}) = 4.75$  and  $\text{pK}_a(\text{ammonium}) = 9.25$ , The initial solution volume was 10 mL for all titration curves.  $\text{H}^+$  and  $\text{OH}^-$  were added as HCl and NaOH, respectively. Modified with permission from ref. [89] (copyright 2013, American Chemical Society).

Figure 1

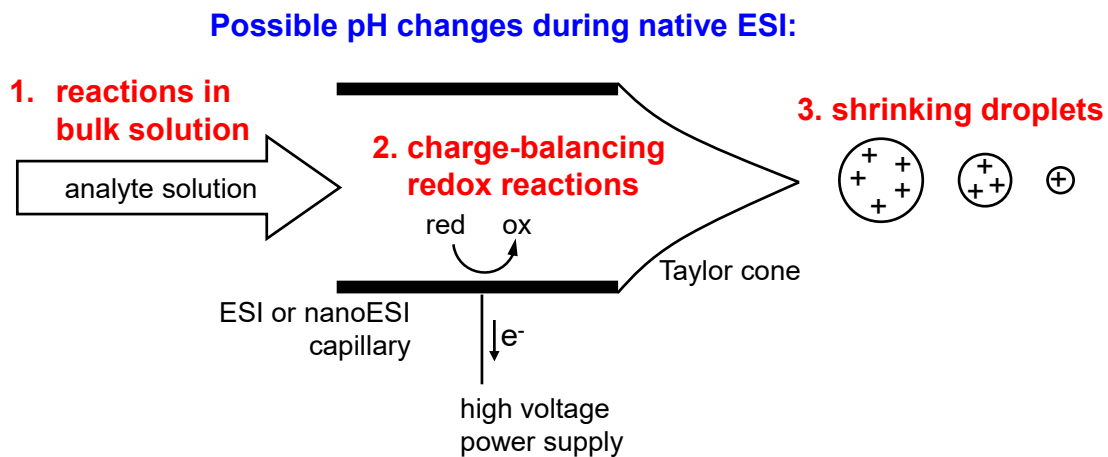


# Figure 2

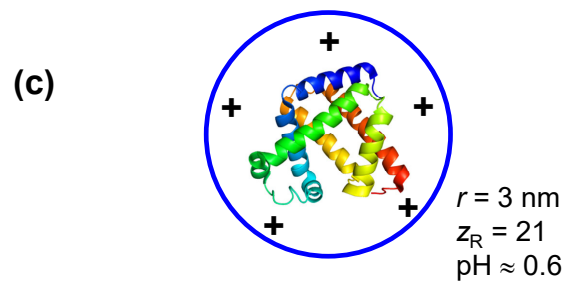
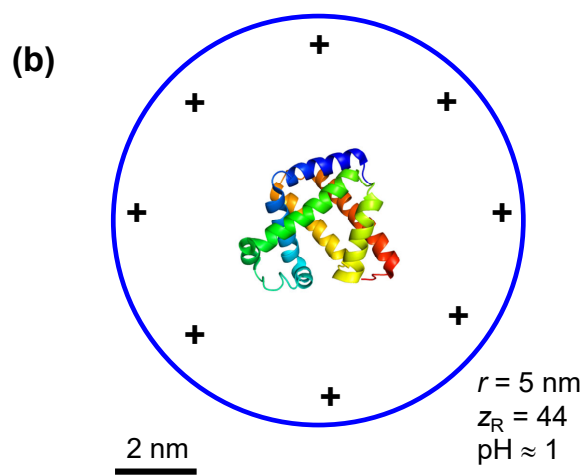
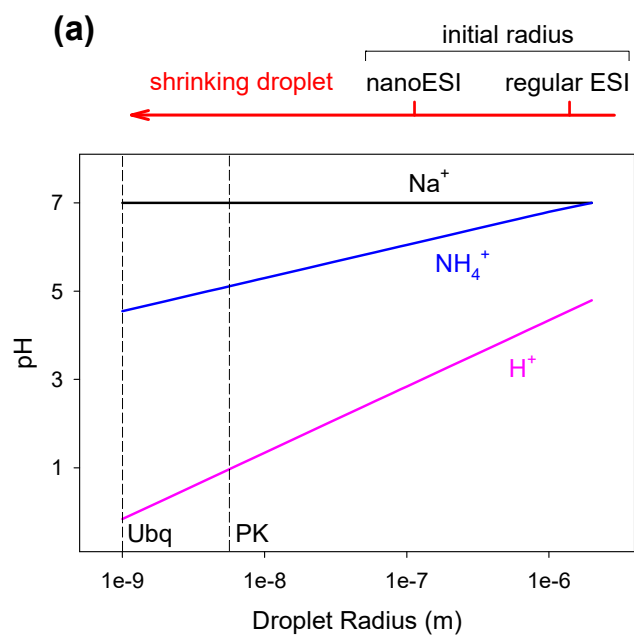
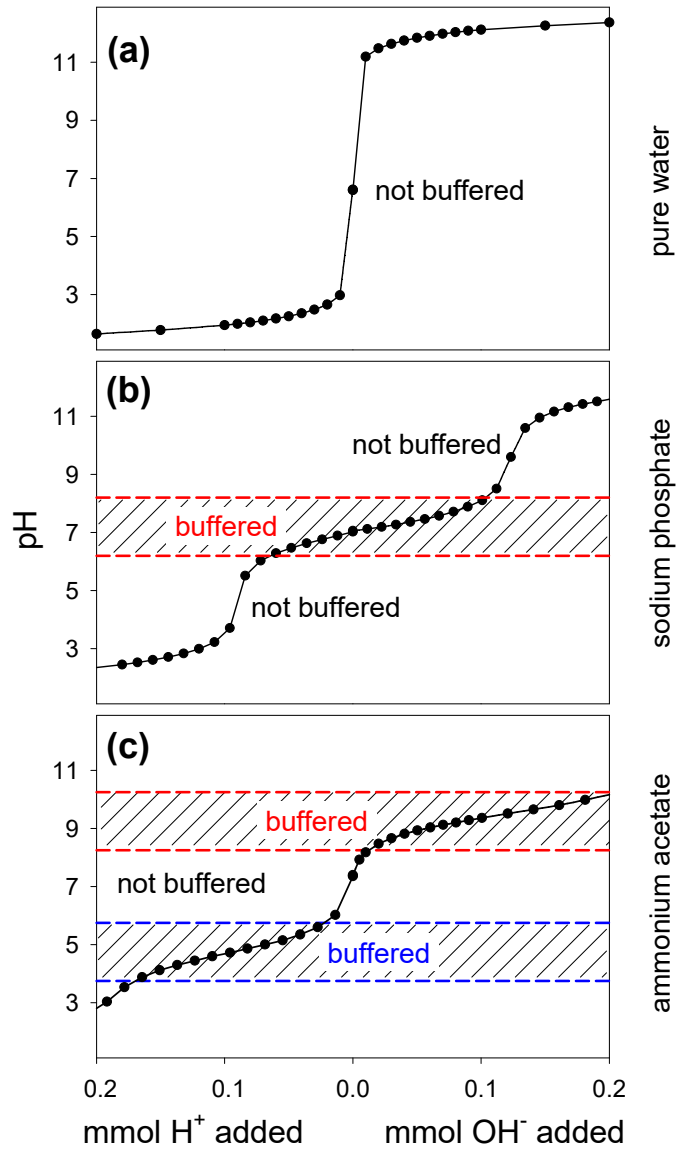


Figure 3



## TOC Figure

